

Anisotropic wetting on structured surfaces

Matthew J. Hancock and Melik C. Demirel

Directional textured surfaces help butterflies to shed water from their wings, pitcher plants to capture prey, and water striders and certain beetles and spiders to walk on water. Inspired by natural directional surfaces, researchers have developed a myriad of synthetic surfaces with precisely tuned physicochemical properties to regulate wettable adhesion. Anisotropic surfaces are of great value to the energy and biomedical fields for applications such as directional syringes, microprocessor cooling, high-efficiency hydropower turbines, and nanoscale digital fluidics. We summarize experimental and theoretical approaches to the design, synthesis, and characterization of engineered surfaces demonstrating anisotropic wetting properties.

Introduction

A broad body of literature has been published in the last decade on anisotropic surfaces exhibiting directional wetting properties (also see the Liu et al. article in this issue).[1–5] We highlight here the most recent additions to this field, including directional membranes, directional electrowetting, directional imbibition, directional checkerboard surfaces, ratchet surfaces, and, finally, recent computational advances to model droplets on chemically and geometrically patterned surfaces.

The term "wetting" refers to the degree to which a liquid can wet a given surface (see the Introductory article in this issue). Anisotropic wetting is the directional dependence of wettability due to asymmetric physical or chemical patterns in a material's surface. To determine the anisotropy of a surface, five factors should be considered: the asymmetry of (1) the structure and geometry; (2) the external field or stress; (3) the boundary conditions (i.e., constraints on the surface); (4) a physical property (i.e., generalized anisotropic constitutive relations), for example the stress-strain relation; and (5) the resulting deformation (**Figure 1**).[4] A recent review on bioinspired directional surfaces classified these variations in detail.[4]

Fabrication and synthesis of anisotropic surfaces

The array of techniques used to fabricate anisotropic surfaces is outlined in **Figure 2**. These techniques can be categorized as (1) rigid structures, (2) stimuli-responsive structures, or (3) adaptive structures. Numerous techniques for manufacturing rigid anisotropic surfaces have been developed, ranging from templated and template-free deposition to photolithography to direct printing (Figure 2a–b).[3–5,51,80,81] Linear grooves produced via direct micro-machining[6] and lithography have produced surfaces with a preferred axis of wetting. Recently, directional membranes were engineered that provided a wettability gradient along the thickness direction that coupled local geometry and chemical contact angles to cause anisotropic liquid penetration.[7] Such directional membranes are potentially useful for fluid control, membrane separation, and advanced fabrics. Contact angles and adhesion may also be altered through electrowetting, which causes a local voltage-induced molecular reorganization near the solid–liquid interface.[8] Such an approach can direct and deform drops when subjected to a constant external driving force such as gravity.[8] Theoretical simulations have shown that electrowetting can modify the shape of the liquid–liquid interface between two dielectric liquids, yielding a fluidic ratchet mechanism that can propel the fluid.[9]

Engineered surfaces exist that change their wetting properties on command or in response to stimuli. Stimuli responsive surfaces[10] can change their physicochemical properties in response to changes in their environment (e.g., pH, temperature, volume stress). In nature, such dynamic surfaces are used by beetles for defense and by water striders to lay eggs via secretion of a biological wax.[2] Fabrication of polymeric stimuli responsive nanofiber or nanotube structures[12] using

Matthew J. Hancock, Broad Institute, Cambridge, MA; hancock@alum.mit.edu
Melik C. Demirel, The Pennsylvania State University; mdemirel@engr.psu.edu
DOI: 10.1557/mrs.2013.102

© 2013 Materials Research Society

https://doi.org/10.1557/mrs.2013.102 Published online by Cambridge University Press

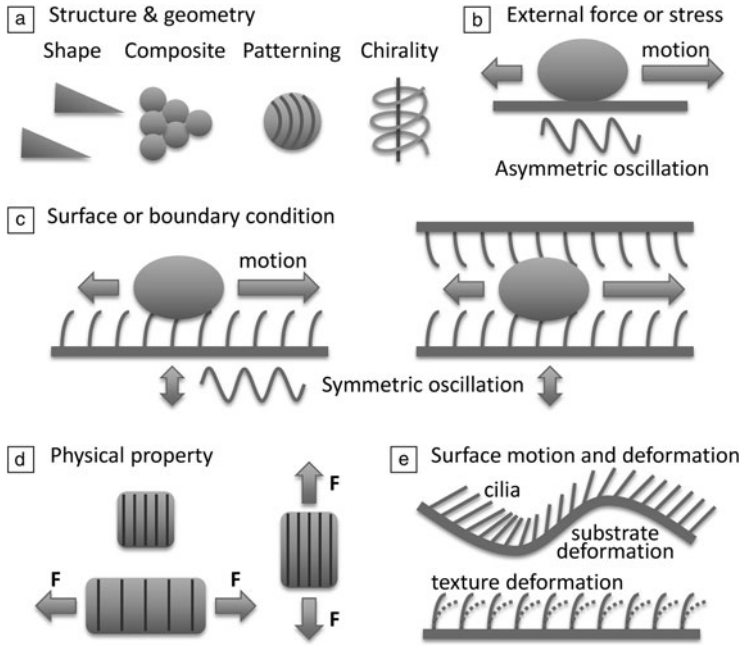


Figure 1. The sources of anisotropy of a surface include the asymmetry of (a) the structure and geometry, (b) the external force or stress, (c) the boundary conditions, (d) the physical property, and (e) the resulting surface motion or deformation. In part (d), the anisotropic physical property could be elasticity, such that when a force **F** is applied in different directions, the spacing of the surface roughness (black lines) changes in different ways. Part (a) is reprinted and (b–d) are adapted with permission from Reference 4. © 2012 Wiley-VCH.

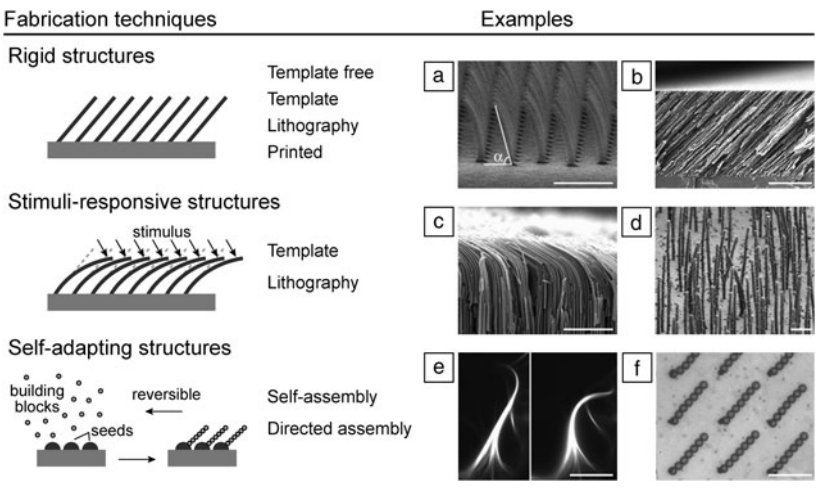


Figure 2. Fabrication techniques for directional surfaces may be categorized as rigid structures, stimuli-responsive structures, and adaptive structures. (a) Polymer coated nano-hairs tilted at an angle α. Reprinted with permission from Reference 80. © 2009 Elsevier. (b) Parylene nanofilms with tilted nanorods acting like nanoratchets. Reprinted with permission from Reference 51. © 2010 Nature Publishing Group. (c) Stimuli-responsive poly(hydroxyethyl methacrylate) nanotubes tilted under shear. See text for details. (d) Magnetically actuated poly(dimethylsiloxane) rods. Reprinted with permission from Reference 20. © 2010 National Academy of Sciences, U.S.A. (e) Cilia-like beating of microtubules assembled with depletion forces on a surface. Reprinted with permission from Reference 78. © 2011 AAAS. (f) Directed self-assembly of spherical superparamagnetic particles in an external magnetic field. Reprinted with permission from Reference 79. © 2010 National Academy of Sciences, U.S.A. Scale bars are (a) 1 μm, (b) 5 μm, (c) 5 μm, (d) 5 μm, (e) 30 μm, and (f) 20 μm.

co-electrospinning[12–14] or template based methods[15–17] have also been reported. Integration of one or more stimuli-responsive polymers into nanostructures could enhance the sophistication of engineered surfaces. The fabrication of directional nanofilms incorporating stimuli responsive polymers is challenging due to the limitations of deposition techniques. Recently, we demonstrated the fabrication of stimuli responsive nanofilms using chemical vapor deposition.[18,19] The nanofilms were fabricated by conformally coating the template membranes with a pH responsive polymer. Specifically, we used vapor deposition of cross-linked poly(hydroxyethyl methacrylate), a pH responsive hydrogel, and sheared the surface to create tilted structures (Figure 2c). Another example of a stimuli-responsive directional surface consists of a soft surface that is powered by external magnetic fields. This surface, which mimics artificial cilia, was fabricated using poly(dimethylsiloxane) and magnetic nanoparticles (Figure 2d).[20]

There is also a great need for assembly approaches to enable rapid and scalable fabrication of self-adapting directional surfaces with predefined geometrical and topographical features and multiple material types. Although self- and directed assembly techniques (Figure 2e–f) were used to fabricate textured surfaces,[78,79] to our knowledge, the number of reports related to directional wetting surfaces incorporating assembly mechanisms is very limited.[21]

Form and function of anisotropic surfaces

A vast amount of literature exists on natural examples of directional surfaces (**Figure 3**). Spider silk collects water via a wet adhesion ratcheting mechanism (Figure 3a–b).[22] After wetting, directional structures form along the silk that create repeating gradients in surface energy and Laplace pressure (i.e., equilibrium pressure difference across an interface) and induce continuous condensation and directional water drop collection.[22] The wings and legs of insects have directional surfaces for thrust generation, drag reduction, water repellency, and water collection.[2,23,24] The desert beetle *Stenocara* sp. uses its bumpy back surface consisting of alternating hydrophobic, wax-coated and hydrophilic, non-waxy regions to capture water from fog-laden wind for drinking (Figure 3c).[25] Butterfly wings have overlapping strips with directed flexible nanoscale tips to allow dew

https://doi.org/10.1557/mrs.2013.102 Published online by Cambridge University Press

or rain droplets to slip off the wing away from the body but not move toward the body (Figure 3d).[26,27] Water strider legs have hairy surfaces with oriented fibers with multiple length scales of roughness to allow them to walk and propel themselves on the free surface of water (Figure 3e–f).[23,28] The adhesive force between the water strider leg and water droplets has been measured in the laboratory (Figure 3g).[24] In the plant world, directional surfaces are used to capture insects and direct rainwater. For example, rice leaves have multiple length scales of roughness to form an anisotropic sliding surface that directs rainwater (Figure 3h).[29,30] The directional leaves on pitcher plants capture, retain, and digest insects, while preventing insect attachment by lubrication of the plant surface (Figure 3i).[31]

A host of research exists on the wetting of chemically patterned surfaces, both in the context of slip and drag reduction[32–36] and adhesion.[4,37,38,60,75] Recent work related to anisotropy includes the experimental study of the anisotropic wetting on checkerboard patterned surfaces, in which central continuous lines present in the patterns strongly influence the trajectories and dynamic wetting of droplets.[44] On the theoretical side, analytical theory combined with dissipative particle dynamics simulations (i.e., a particle based stochastic simulation technique for predicting the dynamics of fluids) predicted the anisotropic flow in a parallel-plate channel with two superhydrophobic striped walls.[45]

A vast volume of literature also exists on the slip and wet adhesion properties of surfaces with geometrical roughness.[32–35,39–43,46–48] Grooved surfaces can exhibit directionally dependent contact angles that result in elongated drops (**Figure 4**a).[49] For non-wetting roughness, ratchet surfaces have been developed to propel drops when heated[50] (Figure 4b) or vibrated; a number of studies exist on microratchet surfaces, as recently reviewed,[4,51] while fewer exist on nanoratchet surfaces.[51,52] Drop motion can persist over long distances, along circular paths, and up or downhill.[53] Specific drop volumes resonate at specific frequencies, providing a means to selectively propel multiple microliter-sized drops,[53] in some cases with cargo, while also enabling drop coalescence (Figure 4c).[52] Drops impacting certain surfaces with directional roughness bounce further with the grain than against (Figure 4d).[4] Moreover, directional roughness can affect the folding of elastic substrates. In Figure 4e, isotropic polymer sheets (poly(dimethylsiloxane), left) and asymmetric parylene sheets (right) were folded by evaporating water droplets.[4] The isotropic and asymmetric sheets folded in symmetric and asymmetric fashions, respectively.[4] This type of capillary driven folding is used by plants to protect their genetic material during times of flooding.

One of the greatest dangers to the stability of elastic fibrous surfaces is clumping due to liquid capillary bridges drawing

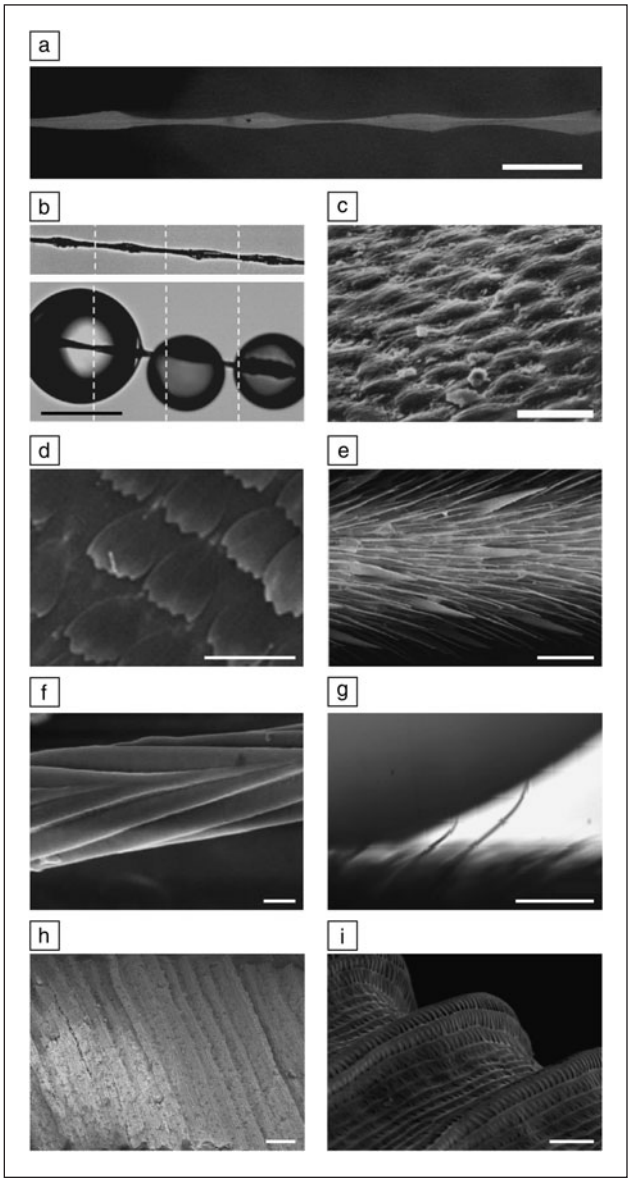


Figure 3. Structured surfaces for anisotropic wetting in nature. (a) Wet-rebuilt silk of the cribellate spider. Scale bar is 50 μm. (b) Water collection on spider silk. Images at initial (top) and later (bottom) times shown. Dashed lines are visual guides linking fixed positions along the silk between the two images. Scale bar is 100 μm. (a–b) Reprinted with permission from Reference 22. © 2010 Nature Publishing Group. (c) The water-capturing surface on the back of a desert beetle *Stenocara* sp. Scale bar is 10 μm. Reprinted with permission from Reference 25. © 2001 Nature Publishing Group. (d) Overlapping microscales on the wings of the butterfly Lepidoptera *Papilio xuthus* (Linnaeus). Scale bar is 100 μm. Reprinted with permission from Reference 27. © 2009 Elsevier. (e) Oriented microsetae on the non-wetting leg of the water strider. Scale bar is 40 μm. (f) Nanoscale grooved structures on a microseta from (e). Scale bar is 400 nm. (e–f) Reprinted with permission from Reference 23. © 2004 Nature Publishing Group. (g) Receding contact line of a droplet moving across the cuticle of a water strider. Scale bar is 100 μm. Reprinted with permission from Reference 24. © 2011 Elsevier. (h) Multiple length scales of roughness on rice leaf surfaces enable anisotropic sliding. Scale bar is 200 μm. Reprinted with permission from Reference 30. © 2011 Wiley-VCH. (i) Surface of peristome (region near mouth) of the *Nepenthes* pitcher plant has two length scales of ridges. Scale bar is 100 μm. Reprinted with permission from Reference 31. © 2004, National Academy of Sciences, U.S.A.

https://doi.org/10.1557/mrs.2013.102 Published online by Cambridge University Press

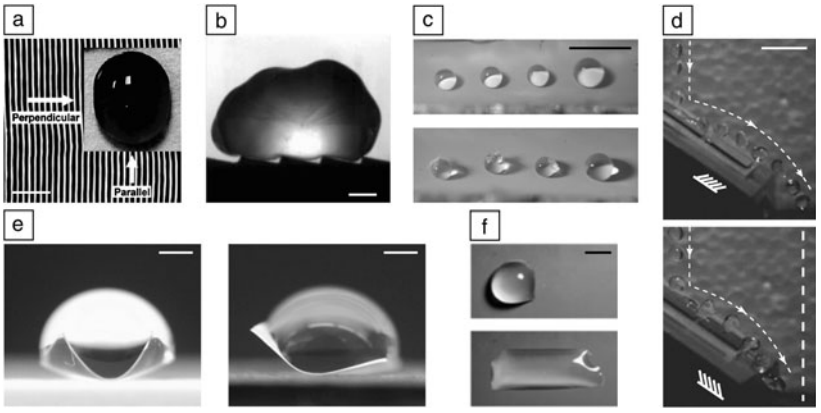


Figure 4. Engineered surfaces with directional wetting properties. (a) Drop elongation on a grooved surface. Scale bar is 2 μm. Reprinted with permission from Reference 49. © 2007 American Chemical Society. (b) Directional milliratchet surface for drop transport by the Leidenfrost effect. Scale bar is 1 mm. Reprinted with permission from Reference 50. © 2011 Nature Publishing Group. (c) Drop transport powered by mechanical vibration on a directional nanorod surface without (top) and with (bottom) cargo (microscale objects). Scale bar is 5 mm. Reprinted with permission from Reference 52. © 2011 American Institute of Physics. (d) Drops impacting a directional surface with the grain (top) bounce further than those impacting against (bottom). Scale bar is 1 cm. Reprinted with permission from Reference 4. © 2012 Wiley-VCH. (e) Polymer sheets coated with isotropic (left) and directional (right) surfaces fold symmetrically and asymmetrically, respectively, by evaporating droplets. Scale bar is 4 mm. Reprinted with permission from Reference 4. © 2012 Wiley-VCH. (f) Directional droplet spreading on a directional nanorod surface. Scale bar is 1 mm. Reprinted with permission from Reference 58. © 2010 Nature Publishing Group.

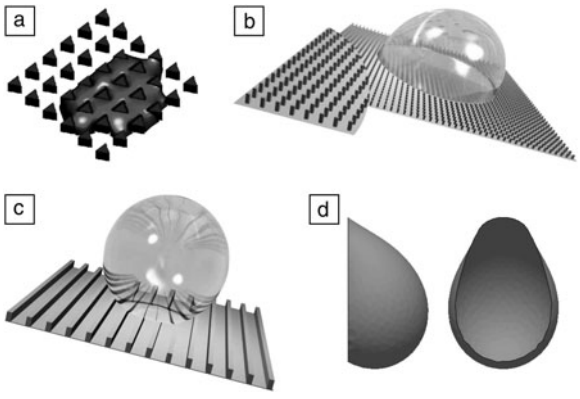


Figure 5. Theoretical simulations of surface wetting. (a) Lattice Boltzmann simulation of liquid spreading directionally through triangular pillars. Reprinted with permission from Reference 62. © 2009 Institute of Physics. (b–c) Lattice Boltzmann simulations of drops on pillared and grooved surfaces, respectively. Adhesion is evident on the pillared surface. Reprinted with permission from Reference 41. © 2007 Springer-Verlag. (d) Side (left) and underside (right) views of Surface Evolver predictions of a drop stuck to a vertical wall by contact angle hysteresis. Reprinted with permission from Reference 72. © 2013 Springer-Verlag. While both the Lattice Boltzmann and Surface Evolver methods must be thoroughly validated against laboratory experiments, they both have great potential to provide efficient estimates of droplet behavior on directional surfaces.

pairs of fibers together with a force per length equal to twice the surface tension.[2,54] The stability of a fibrous array is determined by the fiber rigidity, geometry, capillary force, and droplet volume.[55–57]

A number of experimental studies exist on directing fluids through wettable anisotropic geometrical roughness, called directional imbibition. One such surface uses tilted pillars to induce directional spreading of water droplets (Figure 4f).[58]

A host of approaches have been used to simulate the wetting behavior and motion of droplets and continuous fluid on directional surfaces. For example, a scaling law was recently developed for the dynamics of directional imbibition.[59] Such scaling laws are invaluable to the design of future directional surfaces. Reviews exist for certain popular approaches such as analytic theory, finite element simulations, Lattice Boltzman method (LBM), phase field, and molecular dynamics (MD).[4,60,61] LBM is a popular phase-field diffuse-interface approach that has been used to solve an array of dynamic wetting problems, including imbibition (**Figure 5**a)[62] and droplets sliding on inclined grooved or pillared substrates (Figure 5b–c).[41] At the nanoscale, MD simulations have enabled predictions of the continuous unidirectional flux of water across deformed carbon nanotubes (CNTs) driven by an external oscillating charge without osmotic pressure or a hydrostatic pressure gradient.[63] Other MD simulations have predicted the motion of nanodroplets through CNTs with surface energy gradients.[64]

A surface has inherent contact angle hysteresis (i.e., exhibits contact angles that range between the receding and advancing angle; see the Introductory article in this issue).[65–67] Such hysteresis is responsible for wet adhesion[68,69] and is therefore an important mechanism for designing and fabricating surfaces for directional wet adhesion.[51] The ability to include the advancing and receding angles of each underlying material in a numerical simulation is therefore very important. This issue was recently addressed by incorporating a model for the mobility of the three-phase contact line within Surface Evolver, an easy-to-use public domain finite element package.[70–72] The contact line mobility model was based on a phase field model of surface wetting by sessile drops,[73,74] and its two inputs were the advancing and receding angles of the underlying material. A version of this Surface Evolver model was used to model the advancing and receding of a free surface on a checkerboard pattern,[39] the shape of a pendant drop on a vertical surface just prior to sliding (Figure 5d),[72] equilibrium shapes of coalescing sessile drops on hysteretic surfaces,[72] and coalescing puddles under the influence of gravity and hysteresis.[72] The phase field model itself was

https://doi.org/10.1557/mrs.2013.102 Published online by Cambridge University Press

previously used to study the wetting of a chemical checkerboard pattern where each of the two component materials exhibited hysteresis.[75] Though these recent computational models must still be thoroughly validated against laboratory experiments, they provide a much more computationally efficient method of prediction for a wide range of dynamic wetting problems.

A second challenge with Surface Evolver simulations, and any finite element simulations for that matter, is the parameterization of the patterned surface and solution near it. In the case of Surface Evolver, the solid-liquid interface cannot, in general, be modeled with facets, since individual facets may grow or shrink in order to shortcut the curvature of a hydrophobic solid, while facets may overlap or move over the contact line for hydrophilic solids.[76] To address this issue, the free energy integrals over the solid-liquid surface were converted to line integrals and embedded within the Surface Evolver simulation script to improve the accuracy and convergence of the algorithm.[76] Such an approach allowed the prediction of the Cassie to Wenzel wetting transition (the two main regimes of wetting that occur on structured surfaces) on posts of arbitrary shape, including vertical and inclined posts as well as curved fibers.[76] The simulations showed that curved fibers were more efficient at stabilizing the Cassie state than straight posts. In addition, the simulations yielded important design information, including the location where the interface first depinned.[76]

Summary and outlook

We have summarized recent research on the wetting of anisotropic surfaces by categorizing their fabrication methods, characterizing their anomalous features, and exploring their wide range of applications. Various computational modeling tools are available to predict the directional wetting properties of asymmetric surfaces. New anisotropic surfaces with stimuli-responsive and adaptive features are currently under development. In addition, novel approaches are being developed to enhance the functionality, applicability, characterization, and theoretical modeling of anisotropic wettability.

Directional surfaces not only mimic biological surfaces, but also provide new avenues to discover surface phenomena beyond those in nature. For example, fabrication of adaptive (e.g., self or directed assembly) and stimuli-responsive (e.g., pH, temperature, or magnetic) surfaces will provide novel physicochemical properties in wetting, adhesion, and transport. Nanotextured surfaces made from environmentally friendly materials (e.g., keratin, elastin, laminin, or other elastic proteins) will also be in high demand.[77] Directional surface technology, while still largely confined to laboratory settings, can make a significant impact on the medical and energy fields if these surfaces are integrated into efficient, inexpensive, and environmentally friendly devices.

Acknowledgments

The authors gratefully acknowledge financial support for this work from the National Institutes of Health and The Pennsylvania State University.

References

1. J.W.M. Bush, D.L. Hu, *Annu. Rev. Fluid Mech.* **38**, 339 (2006).
2. J.W.M. Bush, D.L. Hu, M. Prakash, *Adv. Insect Physiol.* **34**, 117 (2007).
3. S.-H. Hsu, K. Woan, W. Sigmund, *Mater. Sci. Eng., R* **72**, 189 (2011).
4. M.J. Hancock, K. Sekeroglu, M.C. Demirel, *Adv. Funct. Mater.* **22**, 2223 (2012).
5. M.K. Kwak, H.-E. Jeong, T.-I. Kim, H. Yoon, K.Y. Suh, *Soft Matter* **6**, 1849 (2010).
6. Z. Yoshimitsu, A. Nakajima, T. Watanabe, K. Hashimoto, *Langmuir* **18**, 5818 (2002).
7. X. Tian, J. Li, X. Wang, *Soft Matter* **8**, 2633 (2012).
8. M. Luo, R. Gupta, J. Frechette, *ACS Appl. Mater. Interfaces* **4**, 890 (2012).
9. K. John, P. Hänggi, U. Thiele, *Soft Matter* **4**, 1183 (2008).
10. I. Tokarev, M. Motornov, S. Minko, *J. Mater. Chem.* **19**, 6932 (2009).
11. A.L. Yarin, E. Zussman, J.H. Wendorff, A. Greiner, *J. Mater. Chem.* **17**, 2585 (2007).
12. Z. Sun, E. Zussman, A.L. Yarin, J.H. Wendorff, A. Greiner, *Adv. Mater.* **15**, 1929 (2003).
13. Y. Dror, W. Salalha, R. Avrahami, E. Zussman, A.L. Yarin, R. Dersch, A. Greiner, J.H. Wendorff, *Small* **3**, 1064 (2007).
14. H. Dong, W.E. Jones Jr., *Langmuir* **22**, 11384 (2006).
15. K.J. Lee, J.H. Oh, Y. Kim, J. Jang, *Chem. Mater.* **18**, 5002 (2006).
16. J. Byun, N.-H. Kim, D.H. Lee, K.-H. Lee, J.K. Kim, *Soft Matter* **5**, 3835 (2009).
17. J. Jang, B. Lim, J. Lee, T. Hyeon, *Chem. Commun.* **83** (2001).
18. G. Ozaydin-Ince, G. Demirel, K.K. Gleason, M.C. Demirel, *Soft Matter* **6**, 1635 (2010).
19. G. Ozaydin-Ince, K.K. Gleason, M.C. Demirel, *Soft Matter* **7**, 638 (2011).
20. A.R. Shields, B.L. Fiser, B.A. Evans, M.R. Falvo, S. Washburn, R. Superfine, *Proc. Natl. Acad. Sci. U.S.A.* **107**, 15670 (2010).
21. D. Xia, L.M. Johnson, G.P. López, *Adv. Mater.* 24 (**10**), 1287 (2012).
22. Y. Zheng, H. Bai, Z. Huang, X. Tian, F.Q. Nie, Y. Zhao, J. Zhai, L. Jiang, *Nature* **463**, 640 (2010).
23. X. Gao, L. Jiang, *Nature* **432**, 36 (2004).
24. M. Prakash, J.W.M. Bush, *Int. J. Non-Linear Mech.* **46**, 607 (2011).
25. A.R. Parker, C.R. Lawrence, *Nature* **414**, 33 (2001).
26. Y.M. Zheng, X.F. Gao, L. Jiang, *Soft Matter* **3**, 178 (2007).
27. D. Byun, J. Hong, Saputra, J.H. Ko, Y.J. Lee, H.C. Park, B.K. Byun, J.R. Lukes, *J. Bionic Eng.* **6**, 63 (2009).
28. X.-Q. Feng, X. Gao, Z. Wu, L. Jiang, Q.-S. Zheng, *Langmuir* **23**, 4892 (2007).
29. J. Gao, Y. Liu, H. Xu, Z. Wang, X. Zhang, *Langmuir* 26, 9673 (2010).
30. D. Wu, J.N. Wang, S.Z. Wu, Q.D. Chen, S. Zhao, H. Zhang, H.B. Sun, L. Jiang, *Adv. Funct. Mater.* **21**, 2927 (2011).
31. H.F. Bohn, W. Federle, *Proc. Natl. Acad. Sci. U.S.A.* **101**, 14138 (2004).
32. J.P. Rothstein, *Annu. Rev. Fluid Mech.* **42**, 89 (2010).
33. E. Lauga, M.P. Brenner, H.A. Stone, in *Handbook of Experimental Fluid Dynamics*, C. Tropea, A. Yarin, J.F. Foss, Eds. (Springer, New York, 2007), p. 1219.
34. L. Bocquet, J.-L. Barrat, *Soft Matter* **3**, 685 (2007).
35. G. McHale, M.I. Newton, N.J. Shirtcliffe, *Soft Matter* **6**, 714 (2010).
36. R. Vellingiri, N. Savva, S. Kalliadasis, *Phys. Rev. E* **84**, 036305 (2011).
37. P.-G. de Gennes, *Rev. Mod. Phys.* **57**, 827 (1985).
38. P.-G. de Gennes, F. Brochard-Wyart, D. Quéré, *Capillarity and Wetting Phenomena: Drops, Bubbles, Pearls, Waves* (Springer, New York, 2004).
39. Y. Kwon, S. Choi, N. Anantharaju, J. Lee, M.V. Panchagnula, N.A. Patankar, *Langmuir* **26**, 17528 (2010).
40. C. Dorrer, J. Rühe, *Langmuir* **23**, 3179 (2007).
41. J. Hyväluoma, A. Koponen, P. Raiskinmäki, J. Timonen, *Eur. Phys. J. E* **23**, 289 (2007).
42. B.M. Mognetti, H. Kusumaatmaja, J.M. Yeomans, *Faraday Discuss.* **146**, 153 (2010).
43. D. Quéré, *Annu. Rev. Mater. Res.* **38**, 16.1 (2008).
44. X. Zhang, Y. Cai, Y. Mi, *Langmuir* **27**, 9630 (2011).
45. J. Zhou, A.V. Belyaev, F. Schmid, O.I. Vinogradova, *J. Chem. Phys.* **136**, 194706 (2012).
46. C. Ybert, C. Barentin, C. Cottin-Bizonne, P. Joseph, L. Bocquet, *Phys. Fluids* **19**, 123601 (2007).
47. A.M.J. Davis, E. Lauga, *Phys. Fluids* **21**, 113101 (2009).
48. A.M.J. Davis, E. Lauga, *J. Fluid Mech.* **661**, 402 (2010).
49. Y. Zhao, Q. Lu, M. Li, X. Li, *Langmuir* **23**, 6212 (2007).
50. G. Lagubeau, M. Le Merrer, C. Clanet, D. Quéré, *Nat. Phys.* **7**, 395 (2011).
51. N.A. Malvadkar, M.J. Hancock, K. Sekeroglu, W.J. Dressick, M.C. Demirel, *Nat. Mater.* **9**, 1023 (2010).

https://doi.org/10.1557/mrs.2013.102 Published online by Cambridge University Press

52. K. Sekeroglu, U.A. Gurkan, U. Demirci, M.C. Demirel, *Appl. Phys. Lett.* **99**, 063703 (2011).
53. T.A. Duncombe, E.Y. Erdem, A. Shastry, R. Baskaran, K.F. Böhringer, *Adv. Mater.* **24**, 1545 (2012).
54. Y.I. Rabinovich, M.S. Esayanur, B.M. Moudgil, *Langmuir* **21**, 10992 (2005).
55. H.-Y. Kim, L. Mahadevan, *J. Fluid Mech.* **548**, 141 (2006).
56. J. Bico, B. Roman, L. Moulin, A. Boudaoud, *Nature* **432**, 690 (2004).
57. C. Duprat, S. Protière, A.Y. Beebe, H. Stone, *Nature* **482**, 510 (2012).
58. K.-H. Chu, R. Xiao, E.N. Wang, *Nat. Mater.* **9**, 413 (2010).
59. N. Obara, K. Okumura, *Phys. Rev. E* **86**, 020601 (2012).
60. H. Kusumaatmaja, J.M. Yeomans, *Langmuir* **23**, 6019 (2007).
61. H. Kusumaatmaja, J.M. Yeomans, in *Simulating Complex Systems by Cellular Automata*, A.G. Hoekstra, J. Kroc, P.M.A. Sloot, Eds. (Springer-Verlag, Berlin, 2010), p. 241.
62. M.L. Blow, H. Kusumaatmaja, J.M. Yeomans, *J. Phys. Condens. Matter* **21**, 464125 (2009).
63. H. Lu, X. Nie, F. Wu, X. Zhou, J. Kou, Y. Xu, Y. Liu, *J. Chem. Phys.* **136**, 174511 (2012).
64. J. Kou, M. Mei, H. Lu, F. Wu, J. Fan, *Phys. Rev. E* **85**, 056301 (2012).
65. R.E. Johnson Jr., R.H. Dettre, in *Advances in Chemistry, Vol. 43: Contact Angle, Wettability, and Adhesion*, F.M. Fowkes, Ed. (American Chemical Society, Washington, DC, 1964), p. 112.
66. R.H. Dettre, R.E. Johnson Jr., in *Advances in Chemistry, Vol. 43: Contact Angle, Wettability, and Adhesion*, F.M. Fowkes, Ed. (American Chemical Society, Washington, DC, 1964), p. 136.
67. R.H. Dettre, R.E. Johnson Jr., *J. Phys. Chem.* **69**, 1507 (1965).
68. E.B. Dussan V, R.T.P. Chow, *J. Fluid Mech.* **137**, 1 (1983).
69. C.W. Extrand, Y. Kumagai, *J. Colloid Interface Sci.* **170**, 515 (1995).
70. K.A. Brakke, *Exp. Math.* **1**, 141 (1992).
71. J. Berthier, K. Brakke, *The Physics of Microdroplets* (Wiley-Scrivener, Hoboken, NJ, 2012).
72. B.R. Prabhala, M.V. Panchagnula, S. Vedantam, *Colloid Polym. Sci.* **291**, 279 (2013).
73. S. Vedantam, M.V. Panchagnula, *Phys. Rev. Lett.* **99**, 176102 (2007).
74. S. Vedantam, M.V. Panchagnula, *J. Colloid Interface Sci.* **321**, 393 (2008).
75. N. Anantharaju, M.V. Panchagnula, S. Vedantam, *Langmuir* **25**, 7410 (2009).
76. M.L. Blow, J.M. Yeomans, *Int. J. Mod. Phys. C* **23**, 1240013 (2012).
77. X. Hu, P. Cebe, A.S. Weiss, F. Omenetto, D.L. Kaplan, *Materials Today* **15**, 208 (2012).
78. T. Sanchez, D. Welch, D. Nicastro, Z. Dogic, *Science* **333**, 456 (2011).
79. M. Vilfan, A. Potočnik, B. Kavčič, N. Osterman, I. Poberaj, A. Vilfan, D. Babič, *Proc. Natl. Acad. Sci. U.S.A.* **107**, 1844 (2010).
80. H. Yoon, H.E. Jeong, T. Kim, T.J. Kang, D. Tahk, K. Char, K.Y. Suh, *Nano Today* **4**, 385 (2009).
81. Y. Yan, N. Gao, W. Barthlott, *Adv. Colloid Interface Sci.* **169**, 80 (2011). □





https://doi.org/10.1557/mrs.2013.102 Published online by Cambridge University Press